# Estimation of forest biomass using L-band backscatter microwave satellite data

Kevin Black[a*], Maarten Nieuwenhuis[b], Fiona Cawkwell[c] and Preethi Balaji[c]

**Abstract**

Synthetic Aperture Radar (SAR) satellite data can be used to monitor spatial and temporal changes in forest biomass and timber volume. Previous research suggest the SAR L-band backscatter signals saturate at a relatively low stand biomass threshold, making the application limited to thicket stage crops. In this study, new biomass and L-band backscatter regression models were developed using procedures to reduce interference due to radar incidence angle and surface moisture and by applying cross-image calibration using both forest and non-forest plot data to increase the biomass saturation point for stand biomass and volume. Many of the widely published model formulations were found not to provide a suitable model fit because of non-normal distribution and evidence of heteroskedasticity of model residuals. The model re-developed in this study performed better than published models, based on lower Akaike Information Criteria values and no heteroskedasticity of model residuals. The backscatter saturation for the re-developed model occurred at biomass values of c. 100 Mg $ha^{-1}$, so accurate determination of biomass using this approach may be limited to immature forest stands. However, the L-band backscatter-biomass model may be suitable to detect changes in forest biomass or volume due to disturbance events.

**Keywords:** *Biomass regression models, Synthetic Aperture Radar, L-band backscatter.*

## Introduction

Aboveground biomass represents an important component of forest carbon (C) and depletion of this C pool due to anthropogenic disturbances such as deforestation or forest degradation can lead to large greenhouse gas emissions. However, assessments of C loss due to deforestation and harvesting are subject to large uncertainties. Use of active remote sensing techniques, such as Synthetic Aperture Radar (SAR), have shown potential for monitoring spatial and temporal changes in forest biomass. Numerous studies have reported on the direct relationship between SAR backscatter signals (i.e. at the bands of longer wavelengths: P (30-100 cm) and L (15-30 cm)) and

[a] FERS Ltd, Forestry Division, 117 East Courtyard, Tullyvale, Cabinteely, Dublin, D18E00.
[b] UCD Forestry, UCD School of Agriculture and Food Science, University College Dublin, Belfield, Dublin 4.
[c] School of Geography, University College Cork, College Road, Cork, T12 YN60.
[*] Corresponding author: kevin.g.black@gmail.com

forest biomass (Ryan et al. 2012, Huang et al. 2015). In particular, full polarimetric SAR provides combinations of different transmitted and received polarisations, such as horizontally transmitted and vertically received backscatter (HV) signals, which have been shown to detect changes in forest biomass up to a saturation level of 100 to 200 Mg C $ha^{-1}$, depending on the SAR wavelength (C, L, P or S bands). L-band data from the PolSAR satellite have been used to monitor forest disturbance and assess biomass in tropical, boreal and sub-tropical regions (Ryan et al. 2012, Robinson et al. 2013).

A number of factors can affect the relationship between forest biomass and L-band backscatter signals, such as radar incidence angle, changes in surface dielectric properties due to moisture and differences in surface roughness. Therefore, numerous cross-image normalisation and adjustment procedures may be required to provide reliable estimates of forest biomass (Huang et al. 2015). Another confounding factor is that L-band signal saturation for forest biomass occurs at 50 to 100 Mg $ha^{-1}$. Typical conifer plantations in Ireland already contain at least 50 Mg $ha^{-1}$ before first thinning events, so L-band signals may not be sensitive enough to detect intermediate harvest events or accurately assess timber volume biomass in mature stands.

Biomass-backscatter regression models have been developed using field measurements and corresponding L-band signal data (Dobson et al. 1991, Huang et al. 2015). Given the non-linear nature of the relationship between the L-band backscatter signal and biomass values, transformation of the data is required in order to simplify the curve-fitting procedure. However, few studies have assessed the effectiveness of such data transformations in terms of overall regression model performance. Moreover, little consideration has been given to the analysis of normality and heteroskedasticity of model residuals to test data transformations, model forms and performance. This may result in a biased estimation of biomass, particularly in the range where L-band signals for biomass are saturated.

In this study, we assessed the performance of biomass and L-band backscatter-regression models to accurately detect changes in biomass due to forest disturbance by a) applying procedures to reduce interference due to variations in radar incidence angle and surface moisture, b) cross image calibration using forest and non-forest plot data to increase the biomass saturation point and c) comparing different data transformations and model formulations.

## Materials and methods

*Study area and SAR data*

The study area covers four different regions of Ireland (Figure 1), representing forest and site types. The soil type across sites varied from wet peatlands in the west to drier mineral soils in the Wicklow mountains in the east. Topography varied from flat lowlands in Kildare and Carlow to mountainous regions in Wicklow and Cork.

The Phased Array-type L-band Synthetic Aperture Radar (PALSAR) on-board the Advanced Land Observation Satellite (ALOS) operated from January 2006 to May 2011 (Rosenqvist et al. 2007). The PALSAR instrument operated at L-band (λ~24 cm) offering fully polarimetric features. The scenes were acquired in Fine Beam Dual-Polarisation (FBD) mode (horizontal transmit and horizontal receive (HH) and horizontal transmit and vertical receive (HV)) from ascending orbits which had a recurrence cycle of 46 days. The incidence angle of each image at scene centre was approximately 38°. To cover the entire study area, two frames of the same acquisition date were acquired. Data were acquired for the summer months of May-June (2007-2010) for this study (Figure 1). The data frames ordered for sites in Cork, Donegal, Wicklow and Mayo included some portions of neighbouring sites as can be seen in Figure 1.

*SAR Pre-processing*

Through the European Space Agency (ESA) Category -1 proposal (Id 17771), single look complex (SLC) products were acquired. PALSAR 1.1 level dual polarised SLC data were multi-looked at one time in range and four times in azimuth direction to create 15 × 15 m pixels. After co-registration of the images, the data were filtered using a DeGrandi multi-temporal speckle filter to reduce speckle. The images were calibrated radiometrically and geometrically and the digital number was converted to decibel (dB) using Eq. 1 from Shimada et al. (2014) and Woodhouse (2006).

$$\gamma^{\circ} = \frac{\sigma^{\circ}}{cos\theta} \quad [1]$$

where, $\gamma^{\circ}$ is the backscattering coefficient normalised with the cosine of the incidence angle, expressed in dB, $\sigma^{\circ}$ (Backscattering coefficient or differential radar cross-section) = $10 \times \log_{10}$ (DN); DN is the pixel digital number value in HH or HV, and $\theta$ is the local incidence angle.

To ensure proper geometric correction of the SAR scenes, an OSi Digital Elevation Model (DEM) of 10 m spatial resolution and many ground control points (GCPs) was used. The scenes were geometrically corrected to the Irish Transverse Mercator (ITM) projection. Terrain-induced distortions such as layover and shadowing were masked off from the images. The local incidence angle (angle between the normal to the backscattering element and the incoming radiation) generated by the DEM was used to identify the layover and shadowed areas, where negative values represented active layover areas and values greater than 90° represented active shadow areas. Finally, the two frames covering each study site were mosaicked. The SAR processing steps were carried out using SARscape 5.0.001 software within an ENVI environment of version 4.8.

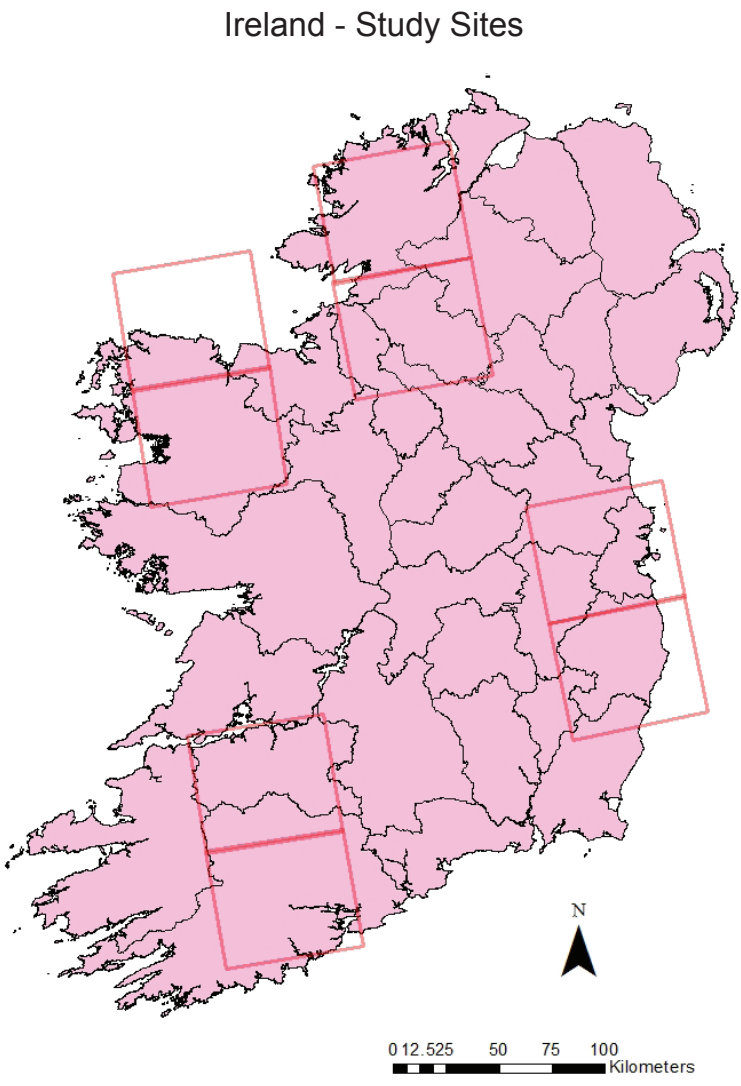


**Figure 1:** *Areas covered by the acquired data frames (red boxes).*

*Correction for incidence angle*

Even after the rigorous radiometric calibration, variations in the backscatter coefficients can be observed. This is due to the dependence of backscatter energy on the incidence angle. To equalise these variations, SARscape applies a cosine correction to the backscattering coefficient in the radiometric correction and normalisation step of the SAR processing. This is based on a modified cosine model by Ulaby and Dobson (1989).

*Correction of backscatter signals for soil moisture and cross image normalisation*

Huang et al. (2015) outlined the sensitivity of the backscatter signals to soil moisture, which masks the biomass-backscatter response, particularly in the biomass value ranges from non-forest to pre-maturity (i.e. before saturation point). The authors propose a two-step normalisation procedure. The first backscatter correction ($\sigma'^{o}_{o}$) makes use of the saturation point of a near-mature forest (S1) relative to the original target backscatter signals from the National Forest Inventory (NFI) ($\sigma^{o}_{o}$) in order to increase the biomass saturation point at higher levels of biomass. The second step normalises the signal ($\sigma''^{o}_{o}$) using the backscatter signals (S2) of both the near-mature forest (S1) and a nearby clearcut area, to reduce the impact of the soil moisture signal by subtracting it from the total signature. Detailed methodologies are outlined by Huang et al. (2105).

Reference clearfelled stands (S2) and mature stands (S1) were selected within a 3 km radius of the target plot (i.e. NFI plot) using Coillte Teoranta's (Irish Forestry Board) forest parcel inventory database. L-band backscatter HV signals for the reference stand were processed and corrected for angle of incidence using the same procedures described in the sections above. Reference stands were selected using the buffer proximity function in ArcGIS v10.2. All S1 stands were selected using a biomass threshold value of 350 Mg ha$^{-1}$, which is well above the backscatter signal saturation point. The status of S1 stands was visually verified using 2011 Bing imagery orthophotographs. It was assumed that a mature stand in 2011 would still have a biomass value well above the signal saturation level of c. 100 Mg ha$^{-1}$ in 2007. The status of S2 stands was verified using Coillte's management and felling records for 2006 and 2007.

*Field data*

Biomass data for target SAR L-band backscatter values in the HV polarisation were derived from the 2007 NFI (Forest Service 2007a). The NFI is based on a random stratified permanent sample system, from which c. 2,000 500 m$^2$ permanent plots are measured for tree and stand metrics. Biomass and timber volume are provided by the NFI (Forest Service 2007b) using biomass algorithms and stem volume equations published by Duffy et al. (2013) and Black (2016). The biomass component represents all aboveground elements including stems, branches and leaves above a stump height of 1% of total tree height. Timber volume was assessed from a stump height of 1% of total tree height to a top end diameter of 7 cm. A total of 450 permanent sample plots were identified in the selected study area, of which 297 were selected for analysis (SAR data were not available for the remainder), which was required when calibration and corrections to the backscatter data were made. A statistical summary of the selected plots is shown in Table 1. The aboveground biomass (AGB) for the

**Table 1:** *A statistical summary of selected plots used for the biomass and volume regression models*.

| Parameter | Mean | Min | Max | N |
|---|---|---|---|---|
| Stocking | 1,124 | 0 | 3,578.0 | 297 |
| Basal area ($m^2$ $ha^{-1}$) | 15 | 0 | 73.0 | 297 |
| DBH (cm) | 22 | 0 | 53.7 | 297 |
| AGB (Mg $ha^{-1}$) | 222 | 0 | 788.0 | 297 |
| Volume ($m^3$ $ha^{-1}$) | 157 | 3 | 650.0 | 207 |

297 plots varied from 0 to 788 Mg $ha^{-1}$. Timber volume was derived for 207 of the 297 plots with a range of 0 to 650 $m^3$ $ha^{-1}$ (50 plots were temporarily unstocked, and 40 contained trees with a DBH less than 7 cm).

*Regression models for biomass mapping*

A range of curve fitting procedures were tested to select the most suitable regression model to predict biomass from the HV backscatter signals. Three curve functions were compared using linear regression analysis and model testing procedures in the R studio package (Venables and Ripley 2002). The first function is the published exponential model (Eq. 2), which describes the non-linear relationship between biomass and backscatter signals (Huang et al. 2015).

$$AGB = e^{a+b\sigma_o^o} \quad [2]$$

where, $AGB$ is aboveground biomass (Mg $ha^{-1}$) and $\sigma_o^o$ is the incidence angle corrected L-band HV backscatter signal (dB). The equation was rearranged to facilitate linear regression modelling (Eq. 3, Model 1).

$$\ln(AGB) = a + b\sigma_o^o \quad [3]$$

The second function (Eq. 4, Model 2) is an inverse exponential model. This is fundamentally different since here AGB is assumed to be proportional to the inverse of $\sigma_o^o$ rather than untransformed $\sigma_o^o$.

$$\ln(AGB) = a + 1/b\sigma_o^o \quad [4]$$

The final model (Eq. 5, Model 3) assumed that the relationship is best described using a hyperbolic function. This best suits the assumption that biomass is fully saturated in mature forest, while exponential functions never reach an asymptote.

$$1/\mathrm{AGB} = a + b(1/\sigma_o^o) \quad [5]$$

To select the best model, a number of goodness of fit parameters were tested, such as root mean square error (RMSE), bias and coefficient of determination ($R^2$). Further regression analysis of predicted and observed values was performed together with a

normality test on model residuals using the Shapiro-Wilk statistic in the R studio. The distribution frequency was considered not to be normal if the p-value of the Shapiro-Wilk estimate was less than 0.05. We also used Akaike Information Criteria (AIC) for model selection to avoid over parameterisation of the model (see Burnham and Anderson 2002), based on the assumption that the lowest AIC values were optimal.

Once the best biomass model was selected, the three separate normalisation and correction backscatter estimators were tested to assess if the signal correction and cross image normalisation procedures improved the prediction of biomass.

Finally, all backscatter variables (i.e. $\sigma^o_o$, $\sigma'^o_o$ and $\sigma''^o_o$) and additional predictors, such as moisture index (SMR), soil nutrient index (SNR), topographical index (TPI), elevation, aspect, slope and radar angle on incidence (RAI) were added to the model using multiple regression modelling in a forward stepwise manner using an R studio (Venables and Ripley 2002). The best model fit was selected based on AIC, with new variables included in the model only when AIC was lower than the initial or last model iteration. The values for SMR, SNR and TPI were derived from an ecological site classification model described for Irish forests by Ray et al. (2009) and Black et al. (2014). The SMR index is based on water holding capacity and SNR is the soil nutrient status of different soil types in the NFI plots. TPI was used as an indicator of topex (Black et al. 2014). These variables were selected because they may influence the backscatter signal and further explain variation in biomass at a given backscatter value.

**Results**

*SAR correction and normalisation*

The angle of incidence corrected SAR L-band backscatter values, in the HV polarisation ($\sigma^o_o$) ranged from -28.22 to -12.82 dB (Table 2). The first step correction ($\sigma'^o_o$) did not have any significant effect on the data structure in terms of the frequency distribution and the range of observed values (Table 2). The cross-image normalisation ($\sigma''^o_o$) did, as it increased the backscatter value range by -1 to 5 dB and skewed the frequency distribution to the right (i.e. higher 3rd quartile percentage and maximum dB values, compared to the non-normalised data, Table 2).

*Biomass model selection*

The first step was to select the best curve fitting procedure using the three models (Eqs. 2, 3 and 4). Goodness of fit estimators showed that model 1 (i.e. the exponential model, Eq. 2) provided the best fit, in terms of the lowest RMSE, bias, AIC and $R^2$ values and the highest F-value from AVOVA (Table 3).

All regressions equations and coefficients were significant at $P < 0.001$. However, the Shapiro-Wilk test on model residuals (i.e. observed minus predicted AGB values)

**Table 2:** *Summary statistics for HV backscatter signals following different correction and normalisation procedures*.

| HV signal | Min. | 1st Qu. | Median | Mean | 3rd Qu. | Max. |
|---|---|---|---|---|---|---|
| $\sigma^o_o$ | -28.22 | -21.09 | -18.22 | -19.05 | -16.82 | -12.82 |
| $\sigma'^o_o$ | -28.66 | -21.34 | -18.63 | -19.27 | -16.94 | -12.71 |
| $\sigma''^o_o$ | -29.20 | -20.92 | -18.10 | -18.83 | -15.48 | -7.45 |

**Table 3:** *Biomass-backscatter curve fit statistics based on the HV backscatter values corrected for angle of incidence ($\sigma^o_o$). F-values for ANOVA and Shapiro-Wilk values for normality tests are significant at P <0.0001 (***).*

| Fit parameter | Model 1 | Model 2 | Model 3 |
|---|---|---|---|
| RMSE | 121.3 | 125.2 | 127.4 |
| Bias | 2.14 | -7.6 | 11.8 |
| $R^2$ | 0.54 | 0.43 | 0.38 |
| F-value | 343 *** | 217 *** | 190 *** |
| AIC | 187 | 195 | 275 |
| Shapiro-Wilk | 0.46 *** | 0.53 *** | 0.85 ** |

suggested that the data were not normally distributed (Table 3). All model residuals also displayed uneven distributions across the observed AGB range, suggesting a problem of heteroskedasticity. For example, plots of Model 1 residuals displayed a fan shaped pattern, characteristic of heteroskedasticity, where residual errors increased as AGB increased (see top right panel in Figure 2). It is also evident that model 1 significantly underestimated biomass at the AGB range above 400 Mg ha$^{-1}$ (Figure 2 top right panel).

In order to further refine the performance of AGB regression model, the angle of incidence corrected backscatter predictive values ($\sigma'^o_o$) used in Model 1 were substituted with the step 1 corrected ($\sigma'^o_o$) and step 2 normalised ($\sigma''^o_o$) values and tested for goodness of fit. Although the 1st step correction ($\sigma''^o_o$) was supposed to increase the backscatter signal saturation point and improve on the AGB prediction, this model did not perform any better than model 1 (Table 3). In contrast, the higher AIC for Model 4 suggested the goodness of fit decreased slightly.

Cross-image normalisation of backscatter for soil moisture did appear to increase model performance (Model 5, Table 4 and Figure 2), when compared to the other models, in terms of a lower AIC and RSME values. Analysis of residuals suggested a non-normal distribution of residuals based on Shapiro-Wilk. Residual plots also show a slight skewing of the frequency distribution, but with no systematic bias in the prediction at high or low observed AGB values (bottom right panel in Figure 2). The residual error for Model 5 also appears to be more normally distributed about the observed AGB data

**Table 4:** *Biomass-backscatter model selection using the best curve fit (Model 1) and different corrected and normalised HV backscatter values. The RMSE and bias estimates are based on the observed and predicted AGB values, not the ln(AGB). F-values for ANOVA and Shapiro-Wilk values for normality tests are significant at P <0.0001 (***), P <0.01(**) and P <0.05(*).*

| | Backscatter value | | |
|---|---|---|---|
| **Fit parameter** | **Model 1** $\sigma^o_o$ | **Model 4** $\sigma'^o_o$ | **Model 5** $\sigma''^o_o$ |
| RMSE | 121.3 | 123.4 | 119.7 |
| Bias | 2.14 | 3.44 | 2.32 |
| $R^2$ | 0.54 | 0.53 | 0.58 |
| F-value | 343 *** | 299 *** | 361 *** |
| AIC | 187 | 199 | 167 |
| Shapiro-Wilk | 0.46 *** | 0.59 *** | 0.38 * |

range, when compared to the scatter plot for Model 1, thus indicating that cross-image normalisation may reduce the occurrence of heteroskedasticity of model residuals.

The final step of the model development was to introduce additional terms into a multiple regression equation to ensure normal distribution of model residuals. Site aspect were also tested in the model because a digital elevation model (DEM) was used to correct backscatter values for angle of incidence. Inclusion of aspect and satellite angle of incidence in the predictive biomass model did not reduce the AIC value so

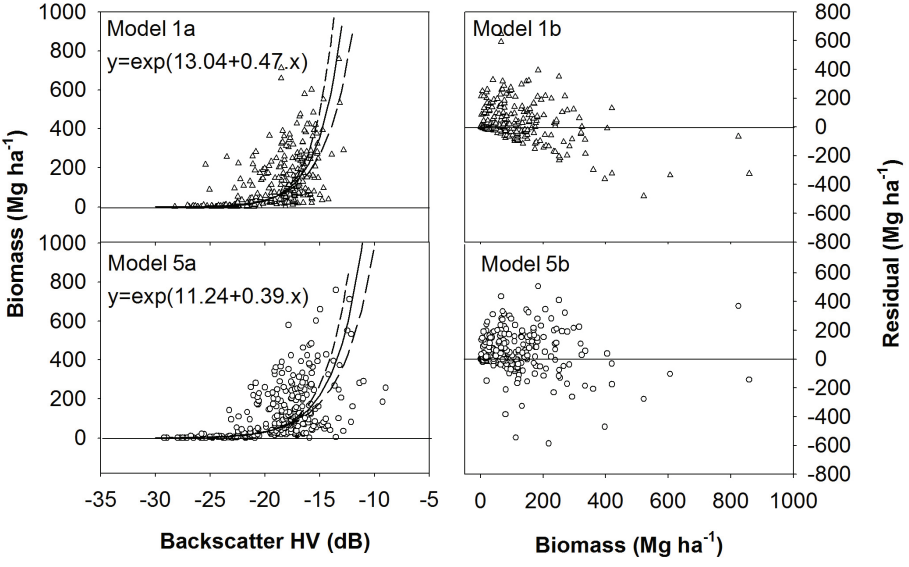


**Figure 2:** *Scatterplots showing the relationship between HV backscatter signals and observed AGB values from NFI plots (left panels, a) and residual versus observed AGB plots (right panels, b) for model 1 and model 5. The solid line plots in the left panels show the fitted regression curves for the models with 95 % confidence intervals (dashed line plots).*

these variables were excluded from the model. A plot of Model 5 residuals against aspect and angle of incidence did confirm that these factors were not contributing to the non-normality (i.e. bias) of model residuals (data not shown).

The final model selection was based on forward model selection using AIC as the selection criteria. The stepwise regression started with Model 1; predictors were then added to the multiple regression in steps provided their addition resulted in a reduction in the model AIC value (Table 5). The final Model (Eq. 6, Model 4) included all backscatter signal correction and normalisation values and the digital elevation (*Alt*, m) of the site, as assessed during the NFI plot surveys:

$$\ln(AGB) = a + b_1\sigma_o^o + b_2\sigma'^o_o + b_{31}\sigma''^o_o + b_4 Alt \quad [6]$$

The same procedure was carried out to develop a predictive model for timber volume (vol, $m^3$ $ha^{-1}$), but the final model produced the best AIC fit with less terms (Eq. 7, Model 5).

$$\ln(vol) = a + b_2\sigma'^o_o + b_3\sigma''^o_o \quad [7]$$

The initial AGB Model 1 had a corresponding AIC value of 187 and the final model produced an AIC value of 158 (Table 5). Addition of the predictors SMR, slope, radar angle of incidence (RAI) and TPI did not improve on model performance (i.e. AIC values were >158).

The final model provided the best estimation of AGB in term of the lowest AIC value. More importantly, all linear regression model assumptions were robust given that model residuals were normally distributed based on the Shapiro Wilk value test (Table 5).

The initial timber volume model used the intercept (*a*) and $\sigma_o^o$ for forward stepwise model selection, resulting in an initial AIC of 36, and a final AIC value of 24 (Model 7, Table 5). However, analysis of residuals for Model 7 suggests a non-normal distribution, indicating that estimation of timber volume is not valid across the observed timber volume range (i.e. the Shapiro-Wilk value was significant, Table 5).

*Detection of clearfell events*

It was not possible to model clearfell events using the NFI data because only three occurred across all of the selected NFI plots over the period 2007 to 2011.

**Discussion**

Huang et al. (2015) used the same model formulations initially used in this study (i.e. Eq. 2) and predicted similar values for the solved coefficients *a* (12.4) and *b* (0.6) using corrected and normalised values from PULSAR HV, when compared to the findings presented in this study (i.e. model 5, Figure 2). They reported a better

**Table 5:** *Fitted coefficients with standard error in parenthesis and performance of the final models (Model 6) for biomass (AGB, Mg ha$^{-1}$) and (Model 5) for timber volume (vol, m$^3$ ha$^{-1}$) using forward stepwise multiple regression. The RMSE and bias estimates are based on the observed and predicted AGB and volume values, not ln(AGB) or ln(vol). F-values for ANOVA and Shapiro-Wilk values for normality tests are significant at P <0.0001 (***) and P <0.01(**).*

| Coefficient/Parameter | ln(AGB), Model 6 | ln(vol), Model 7 |
|---|---|---|
| a | 13.515 (0.571) | 8.041 (0.576) |
| $b_1$ ($\sigma^o_o$) | 0.043 (0.013) | n.s. |
| $b_2$ ($\sigma'^o_o$) | 0.221 (0.077) | 0.066 (0.035) |
| $b_3$ ($\sigma''^o_o$) | 0.218 ( | 0.132 (0.031) |
| $b_4$ (*Alt*) | -1.125E-03(7.65E-04) | n.s. |
| RMSE | 97.4 | 132.0 |
| Bias | 0.61 | 49.10 |
| $R^2$ | 0.61 | 0.17 |
| F-value | 93*** | 24** |
| AIC (initial) | 187 | 36 |
| AIC (final) | 158 | 24 |
| Shapiro-Wilk | 2.70 | 0.94** |

model fit, compared to our model 5 (Table 4), in terms of a higher $R^2$ (0.65) and a lower RMSE (45 Mg ha$^{-1}$). However, Huang et al. (2015) and others (Ryan et al. 2012) provided no information regarding the goodness of fit in terms of model residual analysis. In our study, we found that the widely used model formulation does not provide a suitable fit because of the non-normal distribution of model residuals, and evidence of heteroskedasticity (see Figure 2a, Table 4). The main reasons for heteroskedasticity and a non-normal distribution of model residuals include: a) use of inappropriate model formulations (i.e. selection of unsuitable equation types to suit the data pattern), b) exclusion of predictive variables that may better characterise variations in biomass or c) inadequate data normalisation procedures of model predictors or observed values. Transformation prior to regression analysis and subsequent normality testing of predicted and biomass data and testing of different model formulations confirmed that omission of parameters that are in fact contributing to the variation in the data creates the conditions of bias in the model. Upon visual interpretation of the scatterplot for biomass versus backscatter singles, one may consider that a hyperbolic curve may be a more representative model formulation. However, based on the presented curve fitting comparisons, it is apparent that the widely used exponential curve appears to be most appropriate model to apply (Table 3). The correction for backscatter saturation did not appear to improve model performance, when compared to un-corrected values (Table 4). However, by using the cross-image normalisation procedure proposed by Huang

et al. (2015) and by including additional variables in a multiple regression model, we demonstrated that issues of heteroskedasticity and non-normal distribution of residuals can be resolved (Table 4).

It was not clear if the backscatter interference due to moisture variations were completely resolved using the cross-image normalisation procedure proposed by Huang et al. (2015). This can perhaps be further refined using empirical approaches based on detailed climatic data for all radar scenes and for multiple observations on sampled data from non-forest and mature forest reference sites.

The analysis suggests that HV backscatter corrections for radar angle of incidence may have been adequate because inclusion of the angle of incidence in the multiple regression did not improve model performance. Although the HV signal was corrected for angle of incidence using DEMs, since altitude (*Alt*) was still found to be a significant predictor of biomass from backscatter signals, but it may be suggested that the resolution of the DEM was not sufficient to adequately correct for angle of incidence. Interestingly, the negative slope of the coefficient for *Alt* (see $b_4$ for model 6, Table 5) indicated that stand/site biomass decreased as altitude increased. Such a finding is consistent with currently used forest ecological site classification models (Ray et al. 2009, Black et al. 2016).

Use of L-band backscatter signals to predict forest biomass do not appear to be sufficient to provide precise estimates at the higher ranges (>100 Mg $ha^{-1}$) - as indicated by the high RMSE values, the larger confidence intervals where the backscatter signal saturated and the heteroskedasticity problem for the timber volume model. The model estimates for biomass, developed in this study is consistent with previous suggestion that backscatter saturation occurs at c. 100 Mg $ha^{-1}$ (Figure 2, Ryan et al. 2012), so accurate determination of biomass using this approach may be limited to immature forest stands up to the first thinning stage for conifer crops (stand ages 16-25 years old). It is suggested that use of a longer wavelength P-band may be a more suitable approach to prediction of biomass and volume at higher levels (Dobson et al. 1991). However, L-band backscatter-biomass models may be suitable to detect changes in forest biomass or volume due to clear-felling or catastrophic disturbance events. Unfortunately, this could not be validated in the current study area due to the limited number of NFI plots that were clear-felled between 2007 and 2011.

**Acknowledgements**

The authors would like to acknowledge the Irish Council of Forest Research and Development (COFORD) for funding this research under the CFORREP project (no. 11/C/205).

**References**

Black, K., Creamer, R.E., Xenakis, G. and Cook, S. 2014. Improving the YASSO forest soil carbon model using spatial data and geostatisitical approaches**.** *Geoderma* 232–234: 487–499.

Black, K. 2016. Description, calibration and validation of the CARBWARE single tree-based stand simulator. *Forestry* 86(1): 55-68.

Burnham, K.P. and Anderson, D.R. 2002 *Model Selection and Multimodel Inference: A Practical Information-Theoretic Approach*. 2nd edition Springer-Verlag, New York.

Dobson, M.C., Ulaby, F.T., LeToan, T., Beaudoin, A., Kasischke, E.S. and Christensen, N. 1992. Dependence of radar backscatter on coniferous forest biomass. *IEEE Transactions on Geoscience and Remote Sensing 30*: 412–415.

Duffy, P., Hyde, B., Hanley, E., O'Brien, P., Ponzi, J. and Black, K. 2013. *National Inventory Report; Greenhouse Gas Emissions 1990 – 2011. Reported to the United Nation Framework Convention on Climate Change*. Environmental Protection Agency, Dublin.

Forest Service. 2007a. *National Forest Inventory Republic of Ireland- Methodology.* Forest Service, Department of Agriculture Fisheries and Food. Available at http://www.agriculture.gov.ie/media/migration/forestry/nationalforestinventory/nationalforestinventorypublications/4350NFIMethodology.pdf [Accessed September 2015].

Forest Service. 2007b. *National Forest Inventory Republic of Ireland- Methodology.* Forest Service, Department of Agriculture Fisheries and Food. Available at http://www.agriculture.gov.ie/media/migration/forestry/nationalforestinventory/nationalforestinventorypublications/4350NFIMethodology.pdf [Accessed October 2017].

Huang, W., Sun, G., Ni, W., Zhang, Z. and Dubayah, R. 2015. Sensitivity of multi-source SAR backscatter to changes in forest aboveground biomass. *Remote Sensing* 7: 9587–9609.

Ray, D., Xenakis, G., Tene, A. and Black, K. 2009 Developing a site classification system to assess the impact of climate change on species selection in Ireland. *Irish Forestry* 66: 101–122.

Robinson, C., Saatchi, S., Neumann, M. and Gillespie, T. 2013. Impacts of spatial variability on aboveground biomass estimation from L-band radar in a temperate forest. *Remote Sensing* 5: 1001–1023.

Rosenqvist, A., Shimada, M., Ito, N. and Watanabe, M. 2007. ALOS PALSAR: A pathfinder mission for global-scale monitoring of the environment. IEEE *Transcripts in Geosciences and Remote Sensing* 45: 3307–3316.

Ryan, C.M., Hill, T., Woollen, E., Ghee, C., Mitchard, E., Cassells, G., Grace, J., Woodhouse, I.H. and Williams, M. 2012. Quantifying small-scale deforestation and forest degradation in African woodlands using radar imagery. *Global Change Biology* 18: 243–257.

Shimada, M., Itoh, T., Motooka, T., Watanabe, M., Shiraishi, T., Thapa, R. and Lucas, R. 2014. New global forest/non-forest maps from ALOS PALSAR data (2007–2010). *Remote Sensing of the Environment* 155: 13–31.

Ulaby, F.T. and Dobson, M.C. 1989. *Handbook of Radar Scattering Statistics for Terrain*. Artech House.

Venables W.N., Ripley, B. D. 2002. *Modern Applied Statistics with R.* Fourth edition. Springer.

Woodhouse, I.H. 2006. *Introduction to Microwave Remote Sensing*. Taylor and Francis, Boca Raton.